Reports

Solar Absorption in a Stratosphere Perturbed by NO_x Injection

Abstract. *The changes in the solar absorption by nitrogen dioxide and ozone induced by the injection of* NO_x *(oxides of nitrogen) in the stratosphere are complementary, even though the nitrogen dioxide absorption is only a small fraction of the ozone absorption for an unperturbed stratosphere. The factors causing this effect are described, and an analysis is made of the perturbed solar radiation budget.*

Although much attention has been directed toward NO_2 as a chemical reactant capable of reducing the O_3 layer of the stratosphere (*1*), little attention has been given to its role as an absorber of solar radiation. Solar absorption by NO_2 had not been expected to be significant as compared with solar absorption by O_3 because in many radiative equilibrium models reasonable stratospheric temperature profiles have been generated that did not require the inclusion of NO_2 (*2*). However, as I show here, the increase in solar absorption by NO_2 may be a significant fraction of the decrease in solar absorption by O_3 that occurs after the stratospheric injection of NO_x (oxides of nitrogen).

In the radiative transfer model used for these calculations I have assumed a cloudless, plane-parallel atmosphere in which there is molecular multiple scattering and gaseous absorption above an isotropically scattering ground. The wavelength region between 187.2 and 735 nm, in which O_2, O_3, and NO_2 are the dominant gaseous absorbers, is divided into 119 spectral intervals. The atmosphere between 0 and 55 km is divided into 43 layers, the thickness of a layer being 1 km between 0 and 35 km and 2.5 km between 35 and 55 km. Each atmospheric layer is divided into sublayers such that the optical depth of each sublayer, including scattering and absorption, is less than 0.02. There may be as many as 500 sublayers, depending upon the total optical depth of the atmosphere. The Gauss-Seidel iterative scheme (*3*) is used to solve the radiative transfer equation to obtain the radiative intensity at increments of 6° in the local zenith angle at each level. Components of the radiative intensity are then integrated over solid angle to obtain the diffuse fluxes.

The absorption cross sections were derived from a variety of sources described in (*4*). The vertical profiles of temperature, pressure, and oxygen concentration correspond to those of the *U.S. Standard Atmosphere* (*5*), and the concentration profiles for O_3 and NO_2 were derived from transport-kinetic calculations (*6*).

The two cases considered are NO_x injections (as NO_2) at 17 or 20 km at the rate of 2000 molecule cm^{-3} sec^{-1} uniformly distributed over a 1-km-thick layer. This injection rate (2.5×10^{12} g/year) corresponds to that of a fleet of several thousand supersonic transports (*7*). The stratospheric column densities of O_3 and NO_2 for each of the three cases are shown in Table 1. The unperturbed O_3 profile corresponds to 0.305 atm-cm of O_3. The 17-km injection corresponds (by model calculation) to a 5.3 percent reduction in stratospheric O_3 and a 33.7 percent increase in stratospheric NO_2, whereas the 20-km injection corresponds to an 11.2 percent reduction in O_3 and a 67.5 percent increase in NO_2. In each case, the fractional change in the NO_2 column density is approximately six times the fractional change in the O_3 column density.

Table 1. Stratospheric column densities (above 13 km) for O_3 and NO_2.

Case	O_3 (molecule/cm^2)	NO_2 (molecule/cm^2)
Unperturbed	7.92×10^{18}	4.06×10^{15}
Injection, 17 km	7.50×10^{18}	5.43×10^{15}
Injection, 20 km	7.03×10^{18}	6.80×10^{15}

Table 2. The ratio of the change in NO_2 absorption to the change in O_3 absorption for an a_s value of 0.25.

Case	θ			
	0°	30°	60°	78°
Injection, 17 km	0.38	0.40	0.45	0.50
Injection, 20 km	0.35	0.37	0.41	0.47

For each of the three sets of concentration profiles, O_3 and NO_2 solar absorption rates were computed for values of the solar zenith angle θ ranging from 0° to 78° and values of the surface albedo a_s ranging from 0 to 1. For the unperturbed case, the stratospheric O_3 absorption ranged from 2.95 percent ($\theta = 0°$; $a_s = 0$) to 7.23 percent ($\theta = 78°$; $a_s = 1$) of the incoming solar radiation. For the unperturbed case, the stratospheric NO_2 absorption ranged from 0.072 percent ($\theta = 0°$; $a_s = 0$) to 0.365 percent ($\theta = 78°$; $a_s = 1$) of the solar radiation incident at the top of the atmosphere. This result verifies that the solar absorption by NO_2 is normally only a small fraction (0.024 to 0.050) of the solar absorption by O_3.

The increase in stratospheric solar absorption by NO_2 (with respect to the unperturbed case) as compared with the decrease in absorption by O_3 is given by the ratio $-\Delta A(NO_2)/\Delta A(O_3)$. Values computed for selected values of θ and an a_s value of 0.25 are shown in Table 2. This ratio varies significantly with θ but only slightly with a_s. The ranges of this ratio for the 17- and 20-km injections (Table 2) indicate that the increase in NO_2 absorption significantly compensates for the decrease in O_3 absorption.

There are several factors causing the changes in NO_2 and O_3 absorption to be comparable in the perturbed cases, even though the magnitudes of their separate absorptions are very different in the unperturbed stratosphere. The most significant factor is that the fractional increase in the NO_2 column density is about six times the fractional decrease in the O_3 column density. Other investigators (*8*) have obtained values for this ratio ranging from 4 to 10, depending upon the magnitude and height of the NO_x injection.

Another factor is that the fractional change in O_3 absorption is not identical to the fractional change in the O_3 column density. For the cases considered here, the former is approximately 0.6 times the latter. This effect results from the saturation of the O_3 absorption in the Hartley band (200 to 300 nm). Even with a reduction of 11.2 percent in the O_3 column density, there is virtually no change in the amount of energy absorbed in this band. Most of the change in O_3 absorption occurs in the weaker Huggins (300

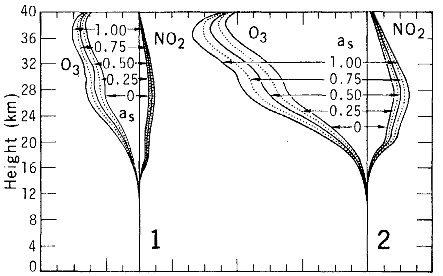

Fig. 1. Changes in O_3 and NO_2 solar heating rates for a θ value of 60° and selected values of a_s: curve 1, 17-km injection; curve 2, 20-km injection.

to 350 nm) and Chappuis (420 to 720 nm) bands. On the other hand, NO_2 absorption occurs primarily in the wavelength region from 300 to 710 nm. The atmosphere is nearly transparent in this spectral region because of the small absorption by other gases. Consequently, sufficient energy is always available for absorption. Thus the controlling factor in NO_2 absorption is the amount of absorber present; as a result, there is near equality between the fractional change in the NO_2 column density and the fractional change in NO_2 absorption.

The ratio of changes in NO_2 and O_3 absorption can be estimated if these factors are combined:

$$-\frac{\Delta A(NO_2)}{\Delta A(O_3)} = \frac{A(NO_2)}{A(O_3)} \times \frac{\left(\dfrac{\Delta NO_2}{NO_2}\right)}{\left(-\dfrac{\Delta O_3}{O_3}\right)} \times \frac{\left[\dfrac{\Delta A(NO_2)/A(NO_2)}{\Delta NO_2/NO_2}\right]}{\left[\dfrac{\Delta A(O_3)/A(O_3)}{\Delta O_3/O_3}\right]} \tag{1}$$

where NO_2 and O_3 are the stratospheric column densities. The first ratio on the right side of Eq. 1 applies to the unperturbed conditions. Substituting values obtained above leads to

$$-\frac{\Delta A(NO_2)}{\Delta A(O_3)} \approx 0.04 \times 6 \times \frac{1}{0.6} \approx 0.4 \tag{2}$$

which is within the range of values shown in Table 2. The first two ratios on the right side of Eq. 1 are determined on the basis of concentration profiles generated from transport-kinetics calculations. These ratios, therefore, are affected by the choice of eddy diffusion coefficients and model chemistry, and the second ratio is affected by the height and magnitude of injection of NO_x. The denominator of the third ratio on the right side depends upon the magnitude of the O_3 reduction. This ratio and the first ratio are also affected to a lesser degree by changes in θ and a_s; thus the potential exists for the ratio of changes in solar absorption to vary over a range greater than that shown in Table 2.

Equation 1 makes it clear why the ratio of the changes in NO_2 and O_3 absorption is nearly the same for the two perturbations. The first and third ratios on the right side of Eq. 1 are not affected by the height of injection of NO_x. Since the changes in the O_3 and NO_2 column densities depend upon the level of injection, only the second ratio is affected. Since the ratio of fractional changes in the NO_2 and O_3 column densities was the same for both perturbations, similar values were obtained for the ratio of changes in absorption rates. Because changes in O_3 and NO_2 absorption occur in the same spectral region (300 to 720 nm), variations in a_s affect similar changes in the absorption rates of NO_2 and O_3. Consequently, the ratio of changes in absorption rates is nearly independent of a_s.

The changes in the instantaneous solar heating rates of O_3 and NO_2 for the 17- and 20-km injections (as compared with the unperturbed case) are shown in Fig. 1 for a θ value of 60° and selected values of a_s. The profiles for the 17- and 20-km injections, although different in magnitude, show similar features. The altitudes at which the maximum changes in the O_3 and NO_2 heating rates occur are well above the level of injection of NO_x for both cases, the maximum change occurring near 37 km for O_3 and near 27 km for NO_2. In the lower stratosphere the changes in the heating rates of O_3 and NO_2 are approximately equal in magnitude, but in the upper stratosphere that of O_3 clearly dominates.

The change in stratospheric composition increases the solar radiation transmitted to the troposphere, resulting in increased tropospheric heating. More radiation is scattered upward from the troposphere, and a larger fraction of this radiation escapes to space because of the increased transmission of the stratosphere, leading to an increase in the planetary albedo and a decrease in the net solar heating of the atmosphere-earth system. An analysis of the perturbed solar radiation budget for the 20-km injection case is shown in Fig. 2 for a θ value of 60°. The increase in stratospheric absorption by NO_2, the increase in tropospheric heating, and the increase in radiation lost to space combine to equal the decrease in stratospheric absorption by O_3. The relative magnitudes of these various components vary with a_s. For small values of a_s, most of the net decrease in stratospheric heating goes into increased tropospheric heating. For large values of a_s, most of the net decrease in stratospheric heating is lost to the system as radiation scattered to space. The increase in NO_2 absorption is approximately a constant fraction of the decrease in O_3 absorption for all values of a_s, as mentioned above.

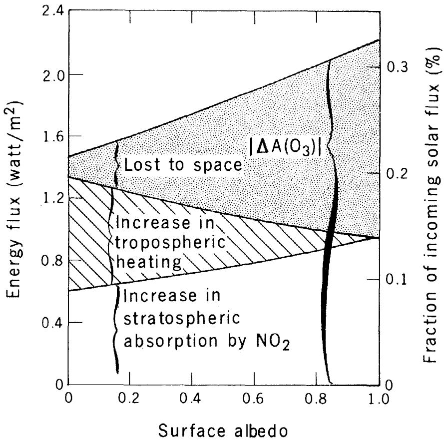

Fig. 2. The decrease in stratospheric absorption by O_3 (upper curve) and the three components that make up this quantity as a function of a_s. This example is for the 20-km injection case and a θ value of 60°.

Although perturbations in the stratospheric composition due to NO_x injection lead to increased solar heating of the troposphere, it does not necessarily follow that these perturbations cause an increase in surface temperature. Perturbations to the longwave (infrared) radiation budget must also be considered when computing changes in surface temperature. Because of the reduction in solar heating of the stratosphere due to the injection of NO_x, the stratospheric temperature will decrease. This reduction in emitting temperature combined with the reduction in O_3 concentration results in a decrease in the downward longwave radiative flux entering the troposphere. This cooling effect tends to counteract the increased solar heating of the troposphere. Ramanathan *et al.* (*9*) found that the longwave effect dominates the solar effect for global mean conditions. Using a radiative-convective model and a perturbation similar to that for the 20-km injection case, they computed a change in surface temperature of −0.1 K.

The fact that a significant fraction of the decrease in net stratospheric heating is lost to the system as radiation scattered to space has important implications for radiative equilibrium models and climatic models dependent on calculations of radiative energy balance. The effect on the planetary albedo of changes in atmospheric composition must be included to accurately compute the perturbed solar radiation budget. The exclusion of the albedo effect may even lead to predicted changes in surface temperature of the wrong sign (*9*). The effect of solar absorption by NO_2 should also be included in these models for case studies involving significant changes in the NO_2 column density.

At biologically important wavelengths in the ultraviolet region (UV-B) (280 to 320 nm), solar absorption by NO_2 has only a small effect on the amount of solar radiation reaching the earth's surface. In this spectral region the optical thickness of O_3 is several orders of magnitude greater than the optical thickness of NO_2; thus the flux of UV-B radiation incident at the earth's surface is much more sensitive to changes in the O_3 column density than to changes in the NO_2 column density. Neglecting solar absorption by NO_2 leads to a slight overestimate of the biological effects from stratospheric injection of NO_x. For the 17- and 20-km injection cases considered above, neglecting solar absorption by NO_2 caused the change in UV-B radiation at the earth's surface to be overestimated by a factor of 1.02.

FREDERICK M. LUTHER
Lawrence Livermore Laboratory,
University of California,
Livermore 94550

References and Notes

1. *Climatic Impact Assessment Program Monograph 3* (Document DOT-TST-75-53, U.S. Department of Transportation, Washington, D.C., 1975); *Climatic Impact Assessment Program Monograph 4* (Document DOT-TST-75-54, U.S. Department of Transportation, Washington, D.C., 1975).
2. For example, S. Manabe and R. Strickler, *J. Atmos. Sci.* **21**, 361 (1964).
3. J. V. Dave and J. Gazdag, *Appl. Opt.* **9**, 1457 (1970).
4. R. Gelinas, *Lawrence Livermore Lab. Rep. UCRL-74944* (1974) (prepared for inclusion in *Climatic Impact Assessment Program Monograph 3*).
5. *U.S. Standard Atmosphere* (Government Printing Office, Washington, D.C., 1962).
6. F. Luther, in *Proceedings of the 4th Climatic Impact Assessment Program Conference*, A. J. Broderick, Ed. (U.S. Department of Transportation, Washington, D.C., in press).
7. *Climatic Impact Assessment Program Report of Findings* (U.S. Department of Transportation, Washington, D.C., 1974).
8. J. Chang and H. Johnston, in *Proceedings of the 3rd Climatic Impact Assessment Program Conference*, A. J. Broderick and G. M. Hard, Eds. (Document DOT-TSC-OST-74-15, U.S. Department of Transportation, Washington, D.C., 1974), pp. 323–329. This paper compares results from several investigators.
9. V. Ramanathan, L. Callis, R. Boughner, in preparation; in *Proceedings of the 4th Climatic Impact Assessment Program Conference*, A. J. Broderick, Ed. (U.S. Department of Transportation, Washington, D.C., in press).
10. I thank Dr. R. Greenstone for first suggesting the importance of NO_2 in the perturbed stratosphere and Dr. J. V. Dave for his guidance and assistance in developing the radiative transfer model. This work was carried out under the auspices of the U.S. Energy Research and Development Administration, under contract W-7505-Eng-48, and was supported in part by the U.S. Department of Transportation High Altitude Pollution Program.

30 September 1975; revised 15 December 1975

Sex Pheromone Specificity in the Pine Sawflies: Interchange of Acid Moieties in an Ester

Abstract. *3,7-Dimethylpentadecan-2-ol was identified as the free alcohol in three species from two genera of pine sawflies (Hymenoptera: Diprionidae). In* Neodiprion lecontei *and* Neodiprion sertifer *the acetate of this alcohol is the major component of their sex attractant; in* Diprion similis *it is the propionate. By examining the responses of the male antennae of several species of* Neodiprion *through the electroantennographic technique, it was determined that four species responded to the acetate and six to the propionate.*

The sawflies, although hymenopterans, have interesting similarities to the moths. Phytophagous cocoon-spinning larvae and nonfeeding adults highly specialized only for reproduction are common to both groups. The females of both groups produce long-range sex attractants (*1*); also, both groups show a multiplicity of closely related species or races adapted to different plant hosts and environments (*2*). In moths, differences in the sex pheromones of closely related species are based on, and restricted to, a few well-defined chemical changes (*3*). The acetate moiety is a conservative feature, although it is sometimes exchanged for an alcohol or aldehyde group. Changes from acetate to propionate or higher esters have not been reported (*4*).

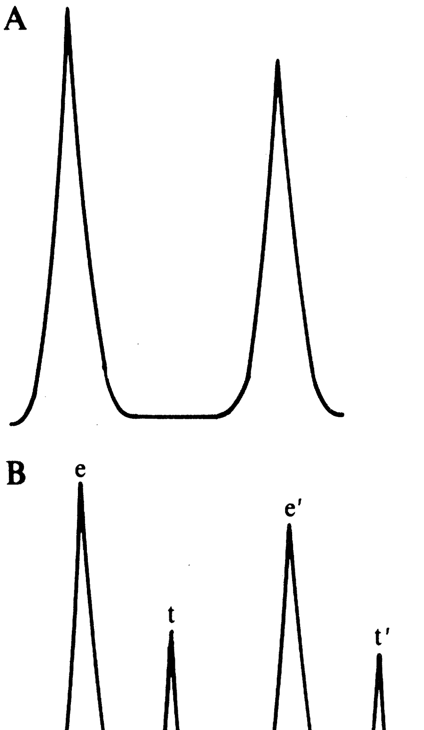

Fig. 1. Juxtaposition of the proton NMR signals for the C-1 methyl group of (A) natural (from *N. sertifer*) and (B) synthetic 3,7-dimethylpentadecan-2-ol acetate, showing that the doublet for the natural product corresponds to the *erythro* diastereoisomer (*ee'*) of the synthetic. The chemical shift, τ, for the latter is 8.91 parts per million, and the coupling constant is 6.5 hertz. The solvent is deuterobenezene.

A genus of pine sawflies, *Neodiprion*, shows exceptional evolutionary diversity; in North America about 30 species or races are adapted to different host conifers (*2*). This diversity provides an opportunity to find out how a group of insects, taxonomically distinct from the Lepidoptera, has solved the common problems of long-range sex attraction and species specificity. The pine sawflies, while conservative in the use of 3,7-dimethylpentadecan-2-ol as the common alcohol moiety, have exploited the interchange of acetate and propionate groups as one means of achieving specificity. Evidence for this is based on chemical identification and on responses by the insects to natural and synthetic esters.

An ether extract was obtained from virgin female *Neodiprion lecontei* by a method already described for *Diprion similis* (*5*). This extract was subjected to short-path distillation, exclusion from a urea complex (*6*), and preparative thin-layer and gas-liquid chromatography (TLC and GLC) (*7*). These procedures, which were monitored by electroantennograms (EAG) (*8*), resulted in the isolation of an active compound that shows a single peak by GLC (*9*). About 4 μg of this compound were obtained from 27,000 insects. Treatment of this compound with potassium hydroxide in methanol produced an inactive neutral compound that has a shorter retention time than the original compound by GLC on an apolar column. Samples of the inactive compound were esterified with formic acid and with the anhydrides of acetic, propionic, butyric, and isobutyric acids in pyridine. After removal of the reagents the samples were tested by EAG. Of the esters so produced, only the acetate was identical to the original active compound as shown by GLC position and EAG activity.

When the remaining (inactive) TLC fractions were acetylated one fraction